

**EFFECT OF REINFORCING PARTICLE MORPHOLOGY ON THE TENSILE RESPONSE OF 6061/SiC/25p DISCONTINUOUSLY-REINFORCED ALUMINUM**

Jonathan E. Spowart<sup>2</sup> and Daniel B Miracle<sup>1</sup>

<sup>1</sup>Air Force Research Laboratory, Materials and Manufacturing Directorate,  
AFRL/MJLLM, Wright-Patterson AFB OH, USA

<sup>2</sup>U.E.S. Inc., Dayton OH, USA

**ABSTRACT**

In order to study the effect of particle morphology on the tensile response and fracture behavior of Discontinuously-Reinforced Aluminum (DRA), two P/M 6061/SiC/25<sub>p</sub> materials were fabricated using established powder blending, compaction and extrusion techniques. One of the materials contained abrasive-grade SiC (F-600) whilst the second material was fabricated using a lower aspect ratio grain, selected to give an overall higher bulk density (HBD) in the as-blended form. Care was taken to ensure that each material contained the same size and volume fraction of SiC particles, and to ensure that each material experienced an identical processing route. Mechanical testing was completed at ambient temperature, in order to measure the effect of particle morphology (F-600 vs. HBD) on both the elastic and plastic tensile response of the DRA. Extensive microstructural and fractographic analyses were also carried out on the as-processed and as-tested specimens, using optical and electron microscopy. Future work includes both analytical and numerical modeling to relate the mechanical behavior to microstructural differences between the two materials.

**KEYWORDS**

Discontinuously-Reinforced Aluminum, DRA, SiC, ductility.

**INTRODUCTION**

Over the last decade, DRA materials based on the Al-SiC or Al-Al<sub>2</sub>O<sub>3</sub> systems have been receiving increasing industrial interest[1, 2]. This can be attributed to more precise process control leading to well-characterized materials with better mechanical properties than those previously available, allowing them to be used in fracture-critical applications for the first time. The currently-available commercial DRA materials show great promise in terms of their specific stiffness (modulus ÷ density) when compared to conventional aluminum alloys, and are therefore seen as excellent candidates for further development as structurally efficient metallic materials. For example, an increase in specific stiffness of 1.5 x can be obtained using a reinforcement volume fraction of 50 %. However, this level of ceramic reinforcement typically reduces the ductility of the DRA around 20–60 % of the ductility of the matrix alloy, as shown in Figure 1.

Evidence from previous studies[3-6] suggests that angular particles can produce high localized hydrostatic stresses in response to external loads, especially at the particle corners. These localized stresses have been linked to void nucleation in the matrix adjacent to the particles during tensile loading. The incorporation of a less-angular reinforcement phase is therefore seen as a potential route to improving the ductility of DRA materials, by reducing the propensity for tensile failure by the commonly-observed void growth and coalescence mechanism. The present work can therefore be considered a first step toward the ultimate goal of producing a more ductile, high specific stiffness DRA.

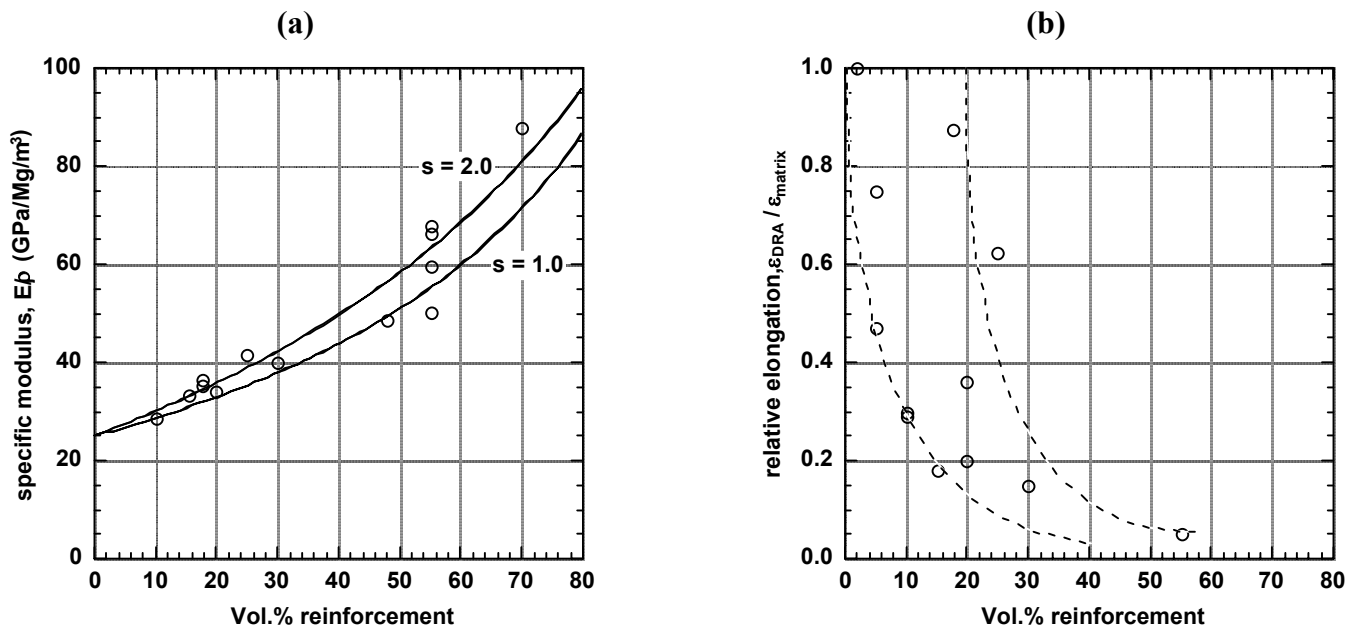


**Fig. 1:** Plot showing: **(a)** specific modulus, and **(b)** relative elongation vs. volume fraction of reinforcement for different DRA materials[7]. Solid lines are from Eshelby-type models[8], based on reinforcement aspect ratios  $s = 1.0$  and  $s = 2.0$ . Broken lines are approximate upper and lower bounds on elongation data.

In order to quantify the effects of particle morphology on the tensile properties of the 6061/SiC/25<sub>p</sub> DRA materials, we required two morphologically different SiC particles. The lower aspect ratio HBD SiC particles used in the present study are produced by a proprietary milling process. The resulting particles have a size distribution similar to the standard abrasive grade F-600 SiC, but with a blocky appearance, Fig. 2. In addition, it is reasonable to conjecture that the HBD particles may have a higher intrinsic strength than the F-600 particles, due to their surviving the mechanical milling process. Both these features are attractive in terms of a ceramic reinforcement for DRA.

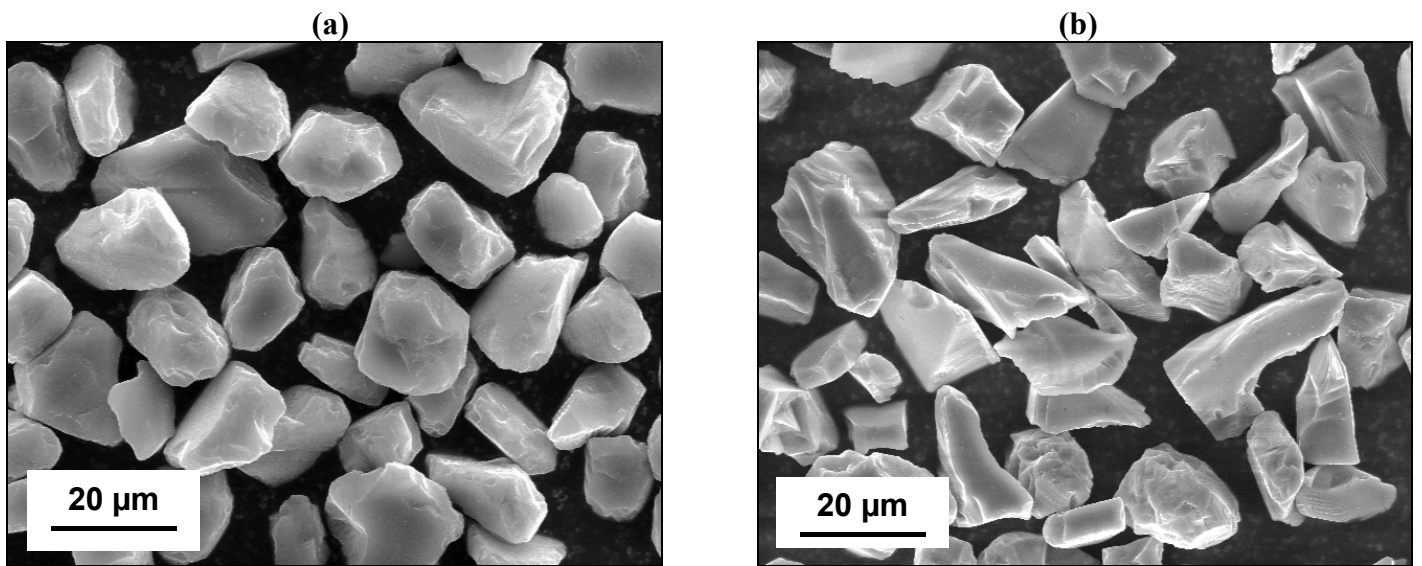


**Fig. 2:** SEM micrographs showing morphology of **(a)** High Bulk Density (HBD), and **(b)** F-600 SiC<sup>1</sup>. In each case, mean particle size  $\approx 12 \mu\text{m}$ .

<sup>1</sup> "Green" SiC powder, obtained from Saint-Gobain Industrial Ceramics, Inc. Worcester, MA.

## EXPERIMENTAL

Al-6061 matrix alloy powders (Al-0.27 Cu-0.26 Fe-0.97 Mg-0.56 Si)<sup>2</sup> were initially screened to -325 mesh prior to blending with the SiC reinforcement. During the blending stage, the matrix and reinforcement powders were suspended in a slurry using 1-butanol as the solvent, in order to reduce agglomeration due to electrostatic forces. After blending, the powders were carefully dried, re-screened to -325 mesh and placed in an extrusion can. An elevated temperature vacuum de-gas treatment was used to remove all traces of residual solvent from the powders, before sealing the cans for compaction and extrusion. Extrusion was carried out at 450°C, with an extrusion ratio of 25:1 (round : round), followed by an air cool (F-temper designation).

Particle aspect ratios were measured from digital micrographs, using a commercial desktop image analysis package<sup>3</sup>. Around 200 particles were selected from each micrograph, at random, in order to perform a statistical analysis of the particle aspect ratios in each material, in both transverse and longitudinal orientations with respect to the extrusion direction. Particle size statistics for the as-received powders were obtained using a Coulter LS 230 Particle Size Analyzer, with small volume unit and associated software. Duplicate samples of each reinforcement were analyzed, using ethanol as the suspension medium.

Room-temperature tensile testing was carried out using a servo-hydraulic test frame under displacement control at a constant strain rate of  $1.3 \times 10^{-4}$ . A flat dog-bone specimen with a gauge length of 25.4 mm was used throughout. The oversize specimen ends were gripped between hydraulic jaws, and a clip-on extensometer was attached to the larger specimen faces for strain measurement. Each specimen was loaded to failure. The two specimen halves were then carefully separated and set aside for examination in SEM.

## RESULTS

### *Microstructural Characterization*

Figures 3(a) and 3(b) show longitudinal sections through each microstructure, with the extrusion direction horizontal. The two microstructures are very similar; especially in terms of the homogeneity of the spatial distribution of SiC particles. However, the F-600 material clearly contains a wider distribution of particle sizes, with many small, angular particles in the section. This qualitative statement agrees well with the particle size analysis results for F-600 SiC ( $d_p = 12.0 \mu\text{m}$ , s.d. =  $4.0 \mu\text{m}$ ) and HBD SiC ( $d_p = 11.5 \mu\text{m}$ , s.d. =  $3.0 \mu\text{m}$ ), in the as-received condition. No obvious porosity was observed in either microstructure.

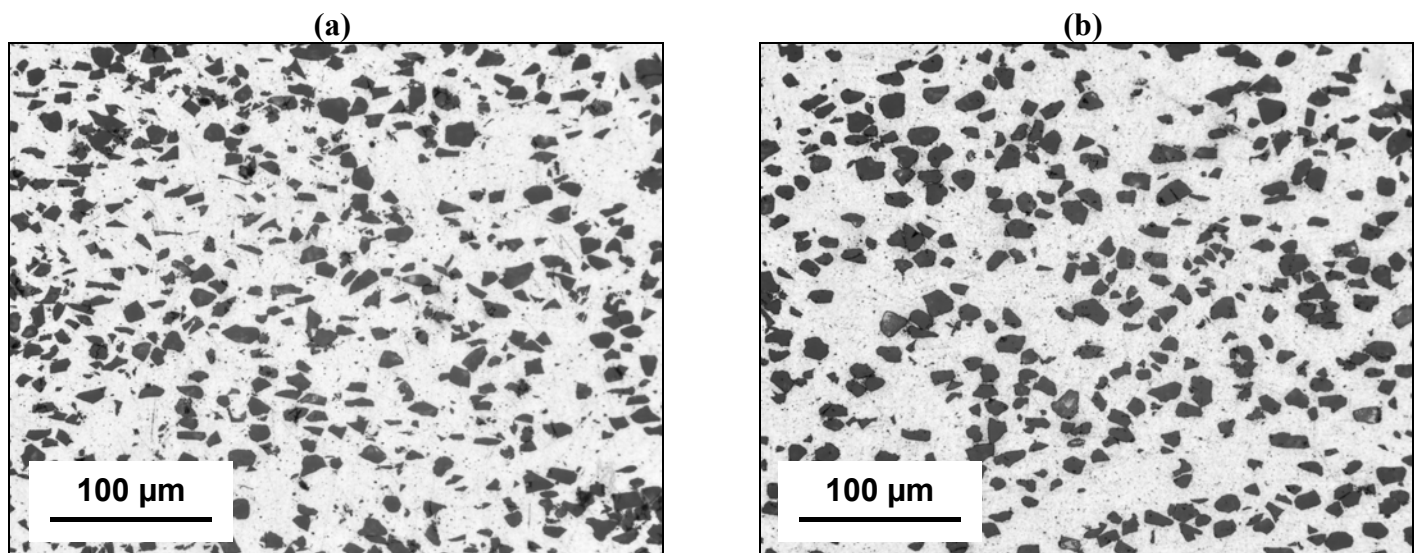


**Fig. 3:** Typical microstructures of (a) F-600 and (b) HBD DRA materials. Longitudinal sections, F-temper, unetched (extrusion direction is horizontal).

<sup>2</sup> spherical gas-atomized 6061-Al powder, obtained from Valimet, Inc. CA.

<sup>3</sup> Adobe Photoshop 5.5, running Image Processing Tool Kit, v2.10.

Figure 4 shows the results of measuring the aspect ratios of 200 particles selected from each of the longitudinal metallographic sections in Figure 3. The F-600 powder has slightly higher mean aspect ratio, with a greater spread in values. However, at these levels of reinforcement (25 Vol %), the effect of the higher particle aspect ratio on tensile properties is expected to be small. For example, interpolating between the curves for  $s = 1.0$  and  $s = 2.0$  on Figure 1(a) gives an increase in tensile modulus of only 3 % on increasing the particle aspect ratio from  $s = 1.6$  to  $s = 1.9$ .

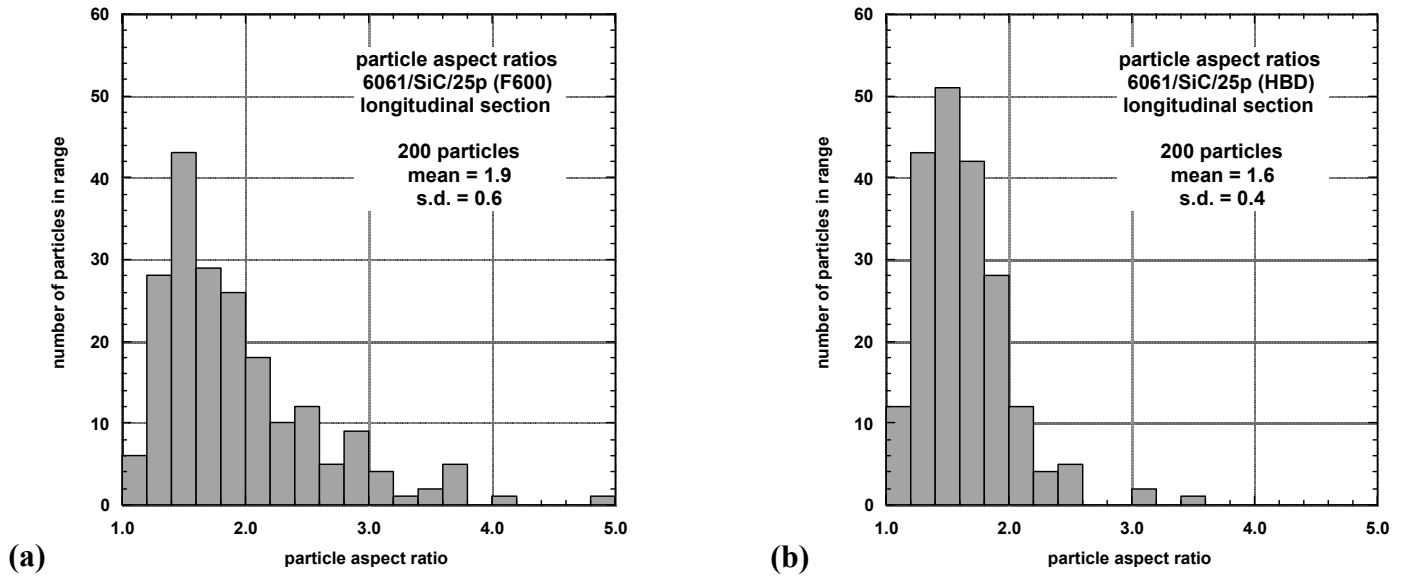


**Fig. 4:** Histograms of particle aspect ratio,  $s$ , for **(a)** F-600 and **(b)** HBD materials, as obtained from longitudinal metallographic sections taken parallel to the extrusion direction.

### Mechanical Behavior

Figure 5 shows representative tensile stress/strain curves for each of the DRA materials. There is only a slight difference between elastic modulus and yield strength values measured in each material, which is well within experimental scatter, as shown in Table 1. However, there is a significant improvement in tensile ductility for the HBD material over the F-600 material. In the F-temper condition, an increase in ductility from 6.6 % to 9.5 % was observed on average, with 3 specimens of each material being tested.

TABLE 1  
TENSILE PROPERTIES OF THE 6061/SiC/25<sub>p</sub> DRA MATERIALS

Material Designation	E (GPa)	$\sigma_Y$ (MPa) <sup>4</sup>	$\sigma_{uts}$ (MPa)	$\epsilon_{ult}$ (%)
6061/SiC/25 <sub>p</sub> (F-600)	$114 \pm 10^5$	$176 \pm 3$	$224 \pm 4$	$6.6 \pm 0.8$
6061/SiC/25 <sub>p</sub> (HBD)	$115 \pm 9$	$173 \pm 2$	$225 \pm 1$	$9.5 \pm 1.6$

### Fractography

Figure 6 shows details of the fracture surfaces of the two DRA materials. The HBD material generally shows a more ductile failure mode than the F-600 material. The HBD SiC particles are largely intact, and often associated with large, deep dimples on the fracture surface, with ductile failure and finer-scale dimpling in the surrounding matrix. Conversely, the lower-relief fracture surface of the F-600 material suggests a more brittle character, with more fractured particles at the surface, and considerable particle debris.

<sup>4</sup> 0.2 % offset yield.

<sup>5</sup> average of 3 specimens,  $\pm$  S.D.

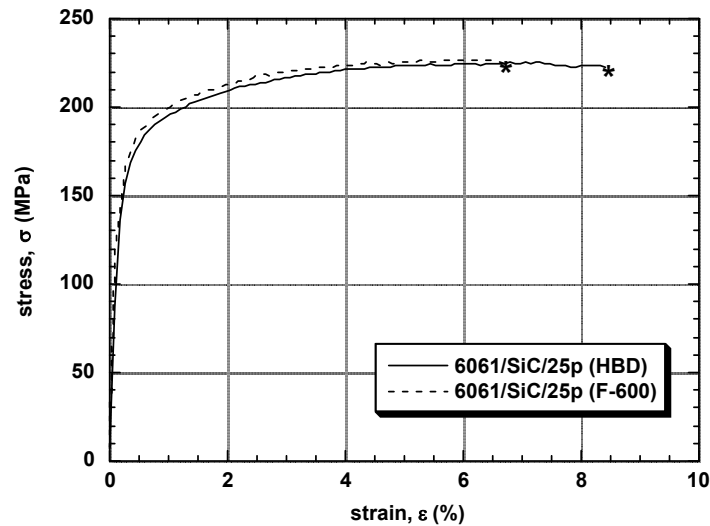


**Fig. 5:** Representative stress-strain curves for the two different 6061/SiC/25<sub>p</sub> DRA materials: solid line, HBD material; broken line, F-600 material. Asterisk indicates failure. Specimens tested in as-fabricated condition (F-temper).

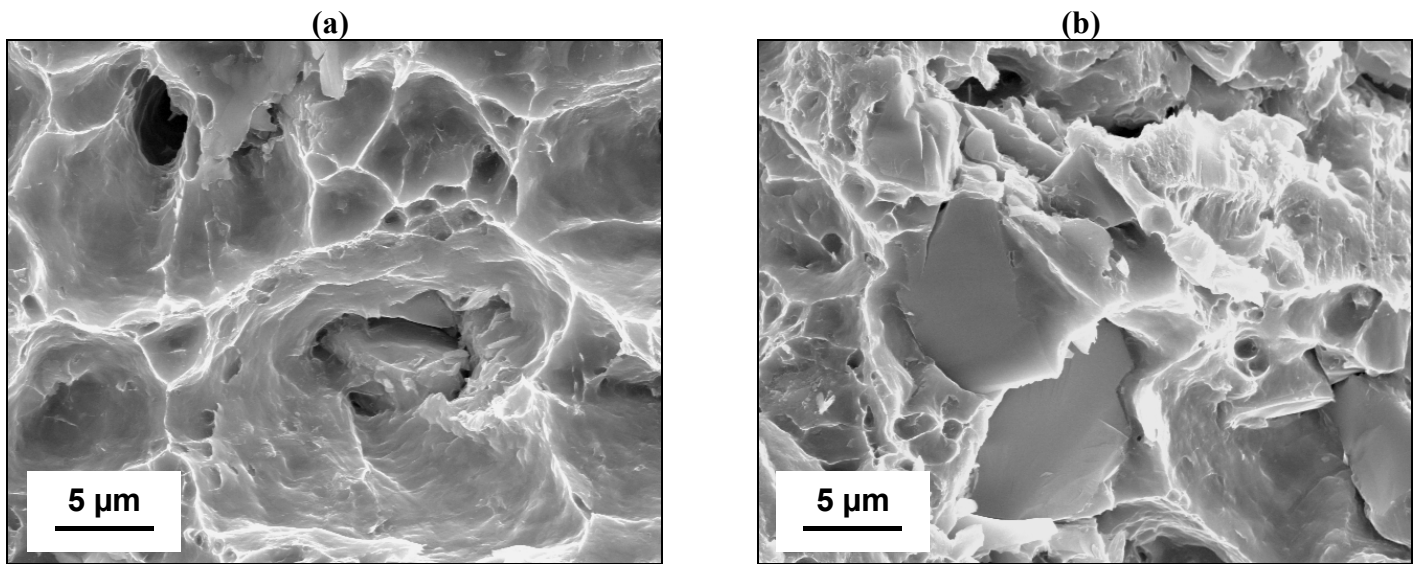


**Fig. 6:** SEM micrographs showing detail of fracture surfaces of DRA tensile specimens: (a) HBD SiC DRA that failed at  $\epsilon_{\text{ult}} = 11.4\%$ , showing extensive matrix plasticity and large dimple associated with SiC particle (b) F-600 SiC DRA that failed at  $\epsilon_{\text{ult}} = 5.7\%$ , showing fractured SiC particles.

## DISCUSSION

In a previous investigation, Song *et al*[9] studied the tensile properties of two different 6061/Al<sub>2</sub>O<sub>3</sub>/20<sub>p</sub> DRA materials. One DRA material was reinforced with angular Al<sub>2</sub>O<sub>3</sub> particles, whilst the other was reinforced with Al<sub>2</sub>O<sub>3</sub>/mullite spheres of a similar size. The spherical particle reinforced material showed a decrease both in elastic modulus and tensile yield strength, compared to the angular reinforcement, however, a marked increase in tensile ductility was also observed. In the present work, however, we observed no decrease in either elastic modulus or yield strength, with a similar increase in ductility for the HBD material. Although our current fractographic investigations are too preliminary to ascertain the precise failure mode(s) operating in each material, there are a number of different mechanisms worth mentioning here. Firstly, the increase in tensile ductility in the HBD material could be attributed to increased strength in the HBD particles

themselves. As the matrix plastic strain increases, load is transferred to the particles, thereby increasing the probability of particle cracking. If the particles are strong, other mechanisms such as interfacial debonding and/or void nucleation and coalescence must occur, at much higher levels of plastic strain. For the more angular F-600 SiC particles, higher localized hydrostatic stresses may exist at the particle corners, thereby increasing the propensity for void nucleation and leading to a lower tensile ductility. We also have the added complication that the weaker F-600 particles may fracture at lower stresses<sup>6</sup> than the HBD particles. The fractured particle fragments can then act as nucleation sites for further matrix voids[5], exacerbating the problem.

It is also worth noting that the results presented here are all based on F-tempered material. Further testing is underway to determine the effect of a peak aging heat treatment on the tensile behavior of the two DRA materials. The addition of a fine dispersion of matrix precipitates should increase the work-hardening rate. Higher matrix flow stresses will lead to higher stresses on the particles at the same level of plastic strain. Whether this in turn leads to a greater improvement in ductility for the HBD material, is a matter for further study.

## ACKNOWLEDGEMENT

This work was supported in part by the Air Force Research Laboratory, Materials and Manufacturing Directorate, under Air Force Contract No. F33615-96-C-5258.

## CONCLUSIONS

- A lower aspect ratio, less-angular SiC particle (HBD) has been identified as a viable reinforcement for experimental high specific stiffness extruded P/M DRA materials.
- Preliminary tensile results show that there is a significant increase in tensile ductility for the HBD SiC DRA compared with the F-600 SiC DRA, with no concomitant loss of elastic modulus, yield strength or ultimate strength.
- Higher tensile ductility in the HBD material may be attributed to either higher strength or less angular morphology of the reinforcement particles.
- The incorporation of HBD SiC reinforcement is therefore seen as a potential route for increasing the ductility of current high specific stiffness DRA materials.
- Further work is planned to ascertain whether the reported increase in ductility is also seen in other heat-treatment conditions, and for different temperatures including cryogenic (LN<sub>2</sub>) temperatures.

## REFERENCES

1. B. Maruyama, W.H. Hunt Jr., JOM 51 1999 59.
2. W.H. Hunt Jr., B. Maruyama, JOM 51 1999 62.
3. T. Christman, A. Needleman, S. Suresh, Acta. Metall. Mater. 37 1989 3029.
4. J.R. Brockenbrough, S. Suresh, H.A. Wienecke, Acta. Metall. Mater. 39 1991 735.
5. A.F. Whitehouse, R.A. Shahani, T.W. Clyne, Metal Matrix Composites: Processing, Microstructure and Properties, 12th RISØ International Symposium, Roskilde, Denmark, 1991, RISØ, 1991, p. 741.
6. H. Luo, R. Ballarini, J.J. Lewandowski, J. Comp. Mats. 26 1992 1945.
7. A. Mortensen, Fabrication of Particulates Reinforced Metal Composites: Proceedings of an International Conference, Montréal, Québec, Canada, 17-24 September, 1990, ASM International, 1990, p. 217.
8. T.W. Clyne, P.J. Withers, An Introduction to Metal Matrix Composites, Cambridge University Press, 1993.
9. S.G. Song, N. Shi, G.T. Gray III, J.A. Roberts, Met. & Mat. Trans. A 27A 1996 3739.
10. P.M. Singh, J.J. Lewandowski, Met. Trans. A 24A 1993 2451.

---

<sup>6</sup> Furthermore, the F-600 particles will experience slightly higher stresses than the HBD particles at the same overall plastic strain, due to more efficient load-sharing at the higher aspect ratios[10].